

NUMERICAL SIMULATION OF PULSED ELECTRIC FIELDS (PEF) PROCESSING FOR CHAMBER DESIGN AND OPTIMISATION

Stefanie SCHROEDER, Roman BUCKOW and Kai KNOERZER

CSIRO – Food and Nutritional Sciences, 671 Sneydes Road, Werribee VIC 3030, Australia

ABSTRACT

The pulsed electric fields technology (PEF) is a highly effective method for liquid food preservation at low or moderate temperatures. One key component of this technology is the treatment chamber, in which the food is exposed to a pulsed electric field. The electric field strength and the temperature distribution in the treatment chamber have been identified as the key processing parameters affecting treatment efficacy and the sensorial characteristic of the food.

A computational fluid dynamics (CFD) model, describing the stationary flow pattern, the electric field and the temperature distributions in a pilot-scale treatment chamber with co-linear configuration of the electrodes, was developed and validated by means of temperature mapping studies using fibre optic probes. The impact of different treatment chamber designs on process uniformity was simulated.

All simulations were performed with the commercial software package COMSOL Multiphysics™ (Comsol AB, Stockholm, Sweden), which is based on the Finite Element Method (FEM).

NOTATION

C_p	isobaric heat capacity [J/kg K]
C_μ	model constant [m^4/kg^4]
d_{in}	internal diameter [mm]
E	electric field strength [V/m]
f	frequency [Hz]
g	gravity constant [$9.8 m/s^2$]
h	height of the gap [mm]
J	current density [A/m^2]
k	turbulent kinetic energy [kg^2/K^2]
k_t	thermal conductivity [W/m K]
k_T	turbulent thermal conductivity [W/m K]
\rightarrow	
n	normal vector
P	pressure including a fluctuating term [Pa]
Q	heat source [W/m^3]
T	temperature [K]
T_{mf}	reference bulk temperature [K]
t	time [s]
\rightarrow	
v	velocity vector [m/s]
\rightarrow	
v_a	averaged velocity vector [m/s]
V	voltage [V]
V_0	maximal potential of pulse [V]
∇	Nabla operator

Greek letters

δ_w	distance from the real wall
ε	dissipation rate of turbulence energy [m^2/K^3]
η	dynamic viscosity [Pa s]
η_T	turbulent viscosity [Pa s]
ρ	density [kg/m^3]
σ	conductivity [S/m]
φ	pulse factor
τ	pulse width [s]
ψ	potential [V]

INTRODUCTION

PEF is commonly understood as a non-thermal food preservation technology that involves the discharge of high voltage electric pulses (up to 70 kV/cm) into the food product, which is placed between two electrodes for a few microseconds (Angersbach et al., 2000). The PEF treatment will compromise the integrity of microbial, plant and animal cell membranes. An external electric field is used to exceed a critical transmembrane potential of one volt. This results in a rapid electric breakdown and conformational changes of cell membranes, which leads to the release of intracellular liquid, and cell death (Hamilton & Sale, 1967). In contrast to conventional heat processing where the energy transfer required to decontaminate liquid food is a limiting factor, PEF shows no time delay in propagating the lethal treatment intensity. However, the degree of microbial inactivation by PEF strongly depends on the properties of the food matrix and processing parameters such as electric field strength and temperature. Electric field strength must be in the range of 20-50 kV/cm with 50-200 kJ/kg energy input (Toepfl & Heinz, 2009). Reportedly, mild heat often has synergistic effects on the PEF treatment efficiency. However, treatment temperature should be kept as low as possible in order to avoid heat damage to the treated product and to prevent off-flavours.

Several studies have shown that PEF can achieve sufficient microbial reduction for liquid food pasteurisation in a wide range of products. However, broad industrial exploitation of this mild preservation process has been held back predominantly due to high operation costs (caused by large amounts of dissipated electric energy).

The uniformity of the process is highly dependent on the specific design of the treatment chamber (Fiala et al., 2001). A uniform treatment can be achieved by a uniform electric field and even temperature distributions, which often require a highly turbulent flow. Several designs have been proposed over the years; mostly known are the parallel, the coaxial and the co-linear configuration (Toepfl et al., 2007). A parallel configuration of the

electrodes allows for a uniform electric field. Other configurations, such as a co-linear configuration, have a less uniform electric field distribution. However, minor modifications of the electrode configuration and isolator geometry can significantly improve the electric field uniformity and turbulent intensity of the flow in the treatment chamber and, thus, result in an enhanced treatment and more even temperature distributions with less pronounced hot spots.

The objective of this study was to develop and validate a specific CFD model describing the stationary flow, the electric field and the temperature distributions inside a pilot-scale PEF treatment chamber with co-linear electrodes arrangement. As it is not feasible to determine such distributions experimentally, the model allows for a better understanding of the critical process points and can be used to estimate the impact of various treatment chamber designs on the treatment uniformity and safety of the process.

MODEL DESCRIPTION

Pulsed Electric Field System

PEF treatment was performed using a Diversified Technologies, Inc. Power Mod™ 25 kW Pulsed Electric Field System, which consists of a PEF-treatment enclosure and a modulator cabinet, an external pump, a heat exchanger, system controls and instrumentations. The System provides “rectangular” pulses with a pulse width in the range of 1-10 μ s, a maximum voltage of 40 kV and a repetition rate of up to 3000 Hz. An example of a pulse provided by the system is shown in Fig. 1.

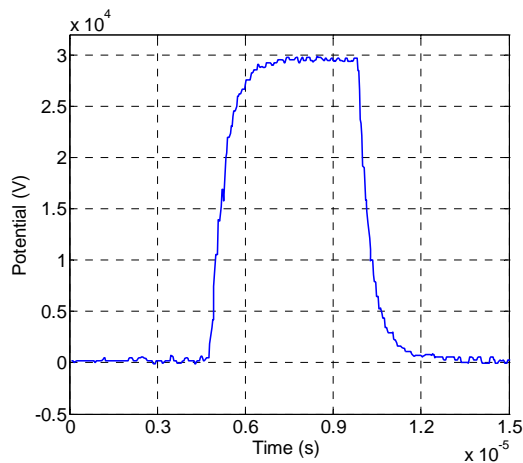


Fig. 1: A typical high voltage pulse with rectangular shape of the modelled PEF system.

Geometry

The geometry of the modelled treatment chamber is shown in Fig.2. The treatment chamber consists of a central high voltage electrode, made of stainless steel, enclosed by two polytetrafluoroethylene (PTFE) isolators and two low voltage (ground) electrodes on both ends.

The considered problem was discretised with the Finite Element Method using triangular grid elements. The mesh was refined, especially in critical regions such as the isolator gap, until no further noticeable changes in model output could be observed.

The model has been designed to be a good approximation of the pilot-scale treatment chamber. As the geometry

comprises only axisymmetric features and no significant difference in the model outcome could be found when comparing full 3D models with axisymmetric 2D models, the axisymmetric representation has been selected for further use (Jaeger et al., 2009). The modelling plane is the r-z-plane, where the horizontal axis represents the r-axis and denotes the radius and the vertical axis represent the z-axis. The modelled system includes two PTFE isolators with an outer diameter of 98 mm and an internal diameter of 16 mm. The overall height of the isolators is 43 mm. Centred along the height of the bore of the isolators, the internal diameter becomes smaller ($d_{in} = 5.15$ mm) forming a spacer (gap; $h = 6.3$ mm) between the high voltage and low voltage electrode. Both, the high voltage electrode, which is centred between the two isolators, and the ground electrodes, have an external diameter of 16 mm and an internal diameter of 5 mm.

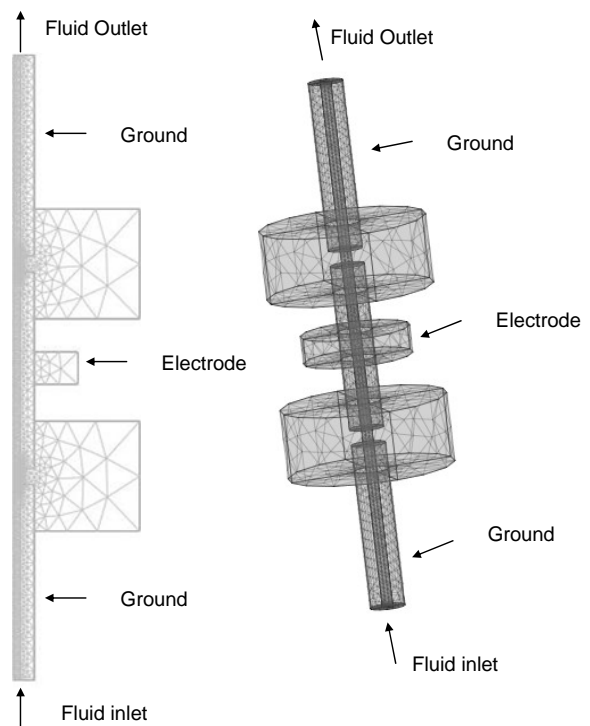


Fig. 2: Co-linear PEF treatment chamber in axis-symmetrical configuration (left) and in full three dimensional configuration (right).

Governing Equations

To accurately model the treatment conditions, three different modules were selected and coupled in COMSOL Multiphysics™, namely, the AC/DC module, describing electrostatic as well as electrodynamic effects, the Chemical Engineering module for describing the laminar and turbulent flow (turbulence by applying the $k-\epsilon$ model) and the Heat Transfer module for solving the energy balance with transport by convection and conduction. The governing equations are adapted from COMSOL.

Governing equations for electrostatics:

Based on charge conservation, the governing equation for the electric potential can be written as

$$\nabla \cdot \vec{J} = \vec{J} \cdot \nabla \cdot (\sigma(T) \cdot \nabla \cdot \Psi) = 0 \quad (1)$$

with \vec{J} denoting the current density and ψ the electric potential.

The relation between the electric field and the electric potential can be described by

$$E = -\nabla \psi \quad (2)$$

where E is the electric field strength.

Governing equations for fluid flow:

The conservation of mass can be described by the continuity equation:

$$\frac{\partial \rho}{\partial t} + \nabla \cdot (\rho \vec{v}) = 0 \quad (3)$$

where ρ is the density of the fluid, t time and \vec{v} the velocity vector.

The calculation of the velocity field is based on the momentum equation:

$$\rho \left[\frac{\partial \vec{v}}{\partial t} + \left(\vec{v} \cdot \nabla \right) \vec{v} \right] = -\nabla P + \nabla \cdot \left(\eta \cdot \nabla \vec{v} \right) + \rho \mathbf{g} \quad (4)$$

where \vec{v} denotes the velocity vector, P includes a fluctuation term, η represents the viscosity and \mathbf{g} the gravity. In turbulence models it is important to account for the nature of the fluctuations around the mean flow. There are certain assumptions about the structure of the turbulence to calculate turbulent fluid. In the Chemical Engineering Module this will be calculated by the Reynolds Averaged Navier Stokes (RANS) equation:

$$\rho \left(\frac{\partial \vec{v}_a}{\partial t} + \left(\vec{v}_a \cdot \nabla \right) \vec{v}_a \right) = -\nabla P + \nabla \cdot \left((\eta + \eta_T) \cdot \nabla \vec{v}_a \right) + \rho \mathbf{g} \quad (5)$$

where \vec{v}_a is the averaged velocity field and P includes a fluctuating term. The only difference compared to the Navier Stokes equation is that η is replaced by $(\eta + \eta_T)$, where η_T is the turbulent viscosity.

The turbulence was solved by applying the k - ϵ model that includes two dependent variables, the turbulent kinetic energy k and the dissipation rate of turbulence energy ϵ . The turbulent viscosity is modelled by

$$\eta_T = \rho C_\mu \frac{k^2}{\epsilon} \quad (6)$$

with C_μ as a model constant.

Governing equations for Heat Transfer

The equation for the energy balance is given by

$$\frac{\partial (\rho \cdot C_p \cdot T)}{\partial t} + \nabla \cdot (\rho \cdot \vec{v} \cdot C_p \cdot T) = Q + \nabla \cdot ((k_1 + k_T) \nabla T) \quad (7)$$

where k is the thermal conductivity, k_T is the turbulent thermal conductivity (including thermal conduction effects from turbulent eddies), C_p is the specific heat capacity and Q denotes an external source of heat, which can be expressed as

$$Q = \sigma \cdot E^2 \quad (8)$$

where E is the electric field strength and σ the media conductivity. For the stationary simulations, the external heat source was multiplied with a factor accounting for the time-averaged potential. The factor φ was determined by relating the averaged high voltage pulse over time to its

maximum value. For simplified rectangular pulses, the factor can be determined with

$$\varphi = \tau \cdot f \quad (9)$$

where τ is the pulse width and f the pulse frequency.

Boundary Conditions

Boundary conditions had to be defined for every application mode. For all modules, symmetry on the centre-axis ($r = 0$) was assumed.

Conductive Media DC

The Conductive Media application mode applies only to the liquid part of the model. For inlet, outlet and isolator gap electric isolation is assumed:

$$\vec{n} \cdot \vec{J} = 0 \quad (10)$$

Electric potential is defined at the high voltage electrode with

$$V = V_0, \quad (11)$$

Where V_0 is the maximum potential of the pulse.

The other electrodes (see Fig. 2) are grounded, i.e. the potential is zero.

$$V = 0 \quad (12)$$

Navier-Stokes Application Mode

A logarithmic wall function is assumed at the inner wall. Turbulence close to the wall is different from isotropic turbulence. There are basically two approaches to account for solid walls subjected to turbulent flow. In the first approach, used for low Reynolds number turbulent models, the equation is modified by additional terms that account for near-wall effects. In the second approach, which is used by this application mode, an empirical relation between the value of the velocity parallel to the wall and wall friction replaces the thin boundary layer near the wall. The logarithmic wall function model is accurate for high Reynolds numbers and assumes that the computational domain begins at a distance δ_w from the real wall.

The inflow velocity boundary condition was assumed to be 5 m/s. A pressure of two bars was defined at the outlet.

General Heat Transfer

This application mode applies to both, the liquid and the solid part of the system. For the inner wall continuity is assumed. Continuity is the default setting for interior boundaries, which applies between any two neighbouring elements.

$$-\vec{n}_u \cdot \left(-(k + k_T)_u \nabla T_u \right) - \vec{n}_d \cdot \left(-(k + k_T)_d \nabla T_d \right) = 0 \quad (13)$$

For the outer wall Heat Flux is applied:

$$-\vec{n} \cdot \left(-(k + k_T) \nabla T \right) = q_0 + h(T_{\text{inf}} - T) \quad (14)$$

At the inlet boundary temperature T_0 is defined, at the outlet convective flux was chosen. This condition states that the only heat transfer is by convection and there is no radiation:

$$-\vec{n} \cdot \left(-k \nabla T \right) = 0 \quad (15)$$

Material Properties

The thermo-physical properties density, specific heat capacity, thermal conductivity and viscosity were obtained from NIST data base (Harvey et al., 1996) as a function of the temperature. The electrical conductivity of

a 50 $\mu\text{mol/L}$ NaCl solution was measured with a conductivity-meter in the temperature range of 4-90 $^{\circ}\text{C}$. These data were fitted in the relevant temperature interval by a polynomial equation and were implemented in the modelling software. The material properties for the electrode ($k = 0.24 \text{ W/mK}$, $\rho = 2200 \text{ kg/m}^3$, $cp = 1050 \text{ J/kgK}$) and the isolators ($k = 44.5 \text{ W/mK}$, $\rho = 7850 \text{ kg/m}^3$, $cp = 475 \text{ J/kgK}$) were taken from the material database already integrated in COMSOL Multiphysics TM.

Process parameters

The chamber was fed with a fully developed fluid flow of 5 m/s, corresponding to a Reynolds number clearly above 25,000, thus the flow was turbulent. The product temperature was conditioned to 300 K at the inlet by using a heat exchanger. In the validation a rectangular pulse was considered with the width of 4 μs (see Fig. 1).

Total specific energy input was chosen to describe the treatment intensity. It was calculated by multiplying the power with the frequency and the pulse duration divided by the flow rate. An estimated energy input could be calculated with 57.6 kJ/L. The temperature increase after the first isolator was estimated to 7 K.

Experimental Validation

A NaCl solution (50 $\mu\text{mol/L}$) was used as model fluid for the experiments. Temperature measurements at two different heights above the second isolator were performed with a fibre optic thermometer inserted into the treatment chamber as well as in two radial locations in both isolators. The experiments were performed under the same conditions as the numerical assumptions.

RESULTS

Fig. 4-6 (a) show the simulations of the pilot scale treatment chamber and PEF system with respect to distributions of the electric field strength, turbulent kinetic energy and temperature, respectively. For the sake of clarity, only half of the treatment chamber is presented (due to axisymmetry). The predicted temperature increase and distribution showed very good agreements with actual measurements at six different locations of the treatment chamber (Fig. 3).

CFD models of four PEF treatment chambers with modified isolator geometries were developed and are shown in Fig. 4-6 (b), (c), (d), and (e). The treatment chamber design consisted of an experimentally validated geometry with co-linear electrode configuration (a). The simulation requires the coupled solution of the governing equations for the electric field, the temperature and the fluid flow as described above.

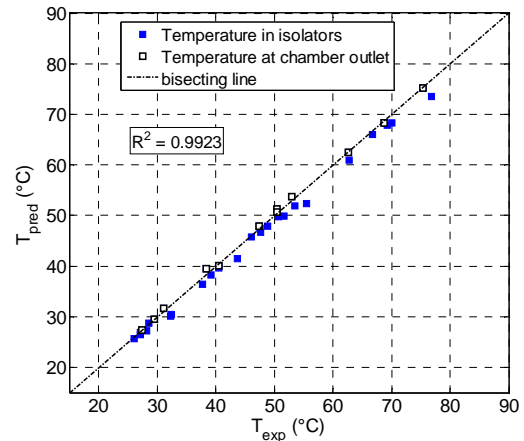


Fig. 3: Correlation of experimental and predicted temperature values at all six fibre optic thermocouple locations.

Impact of the isolator geometry on the electric field distribution

The simulations showed that the electric field distribution is significantly changed by the geometry of the isolator (Fig. 4). It is obvious that the insertion of the isolator in the treatment zone can increase the average electric field strength, and improve the treatment homogeneity.

In the standard chamber (Fig. 4 (a)), the electric field is very non-uniform which is characterised by a high field intensity at the edges and a low field intensity in the centre of the isolators. The reduction of the inner diameter of the isolator (Fig. 4 (b)) bore slightly improves the homogeneity of the field, but still shows intensity peaks at the isolator edges. Rounded isolator edges (Fig 4 (c)) significantly improved the distribution of the electric field. Further improvements of the uniformity of the electric field were found by modifying the treatment chamber according to the geometry shown in Fig. 4 (e), where the isolator has an elliptical form.

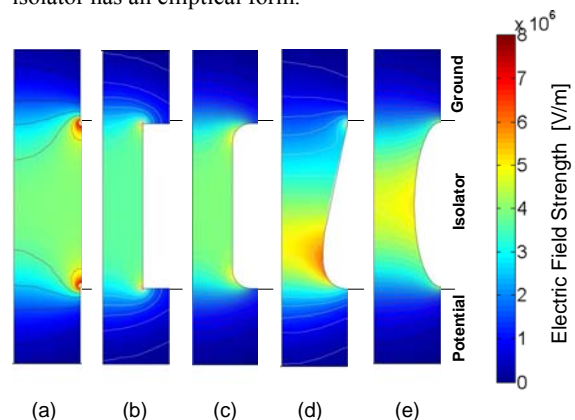


Fig. 4: Predicted distribution of the electric field strength in one half of the treatment chamber for five different isolator geometries.

Impact of the isolator geometry on the flow characteristics

Turbulence is an important attribute in PEF processing as it allows a good mixing of the fluid and thus reduces the temperature non-uniformities and levels in the chamber.

Fig. 5 shows the predicted distribution of the turbulent kinetic energy in the treatment chamber (a) for the current chamber as well as for the modified chamber geometries.

The flow velocity generally peaks on the axis and decrease towards the wall of the treatment chamber. In all scenarios, the fluid enters the chamber at the base with high velocity (5 m/s). Expectedly, chamber design (a) causes the least turbulence as, compared to the other geometries, the isolator does not reduce the pipe diameter and thus leads to increased velocities and Reynolds numbers. The turbulence intensity drastically increases to $18 \text{ m}^2/\text{s}^2$ when the diameter of the isolator is reduced to 3 mm as shown in Fig. 5 (b). However, non-uniformity of the turbulence occurs due to the sharp edges. Rounded isolator edges as in Fig. 5 (c) provide better uniformity of the turbulence but there are still zones in the chamber where the mixing of the media is poor due to flow recirculation areas. An elliptical isolator geometry (Fig. 5 (d) and (e)) gives a more uniform pattern of the turbulent kinetic energy and avoids dead zones of poor media mixing.

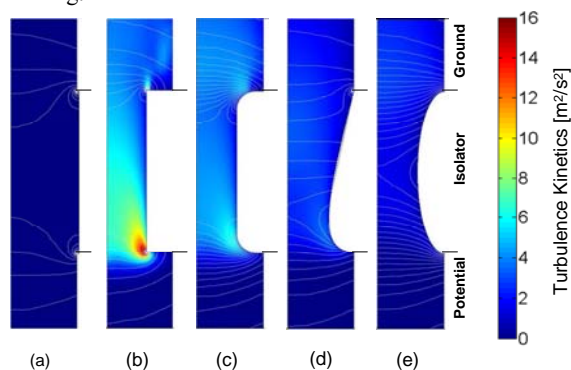


Fig. 5: Predicted distribution of the turbulent kinetic energy in the lower (first) half of the treatment chamber for five different isolator geometries.

Impact of the isolator geometry on the temperature distribution

The knowledge of the temperature distribution is critical for an efficient PEF treatment and largely depends on the distribution of the electric field and the turbulence pattern in the chamber. Thus, it is not surprising that the temperature distribution and the heating of the media in the treatment chamber are depending on the isolator geometry (Fig. 6). The heating of the liquid is highest in treatment chamber geometry (a) which is largely due to the heterogenic electric field and the low turbulence. Very high field strengths at the edges of the isolator cause a drastic heating of the media, which in turn increases the conductivity of the media and thus the energy input in this spot. This phenomenon is known as thermal runaway heating. The low turbulence in this chamber causes the fluid near the wall to move with lower velocity than in the centre of the pipe. This leads to an enhanced heating of the media near the chamber wall and subsequently an increased temperature of the isolators and electrodes due to conduction heating.

At stationary conditions, the total temperature increase with the isolator geometry in our current system is 21 K. In contrast, geometry (b) cause a total heating of 6 K in the media only which is mainly due to the high turbulence kinetic energy observed (Fig. 5 (b)). Whereas the heating of the media is similar in the chamber with isolator geometry (b) and (c), the total temperature increase in scenario (d) and (e) is higher with approximately 12 K and 9 K, respectively. Although the turbulence in these

treatment chambers is less pronounced than in (b) and (c), these isolator geometries allow for a homogeneous electric field distribution and thus for a uniform PEF treatment. It is likely that the energy input required to inactivate microorganisms in these chambers is significantly lower compared to chambers (a), (b) and (c) and therefore should be considered for the PEF pasteurisation of liquid food.

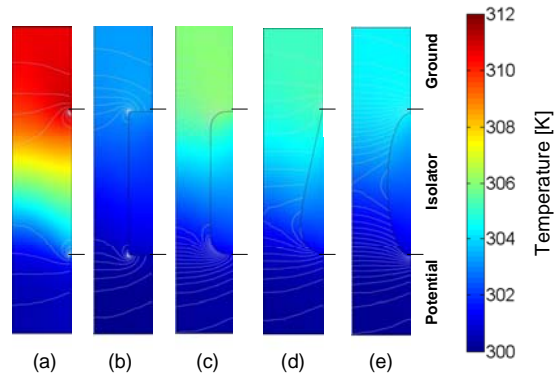


Fig 6: Predicted temperature distribution in the lower (first) half of the treatment chamber for five different isolator geometries.

CONCLUSION

The developed CFD models for a PEF treatment chamber with co-linear electrode configuration but slightly modified isolator geometries have revealed significant differences regarding treatment uniformity and intensity. The standard chamber geometry for PEF pasteurisation of liquid foods showed a very inhomogeneous electric field and poor mixing patterns of the fluid leading to local hot spots and a strong temperature increase due to thermal runaway heating. A reduction of the isolator's inner diameter combined with rounded edges or an elliptical shape significantly improved the uniformity of the electric field and the turbulence pattern of the flow. Numerical simulations showed that small modifications of the isolator geometry can reduce the temperature increase in the treated media by up to 70 %. This would decrease detrimental effects on the nutritional and sensorial characteristics of the treated food and possibly allows for a more energy efficient operation of the process.

REFERENCES

- Angersbach, A., HEINZ, V. & KNORR, D. (2000) Effects of pulsed electric fields on cell membranes in real food systems. *Innovative Food Science & Emerging Technologies*, 1(2), 135-149.
- FIALA, A., WOUTERS, P. C., VAN DEN BOSCH, E. & CREYGHTON, Y. L. M. (2001) Coupled electrical-fluid model of pulsed electric field treatment in a model food system. *Innovative Food Science & Emerging Technologies*, 2(4), 229-238.
- HAMILTON, W. A. & SALE, A. J. H. (1967) Effects of high electric fields on microorganisms: Ii. Mechanism of action of the lethal effect. *Biochimica et Biophysica Acta (BBA) - General Subjects*, 148(3), 789-800.

JAEGER, H., MENESES, N. & KNORR, D. (2009) Impact of pef treatment inhomogeneity such as electric field distribution, flow characteristics and temperature effects on the inactivation of e. Coli and milk alkaline phosphatase. *Innovative Food Science & Emerging Technologies*, 10(4), 470-480.

TOEPFL, S., HEINZ, V. & KNORR, D. (2007) High intensity pulsed electric fields applied for food preservation. *Chemical Engineering and Processing*, 46(6), 537-546.